Analytical time constant design for jerk-limited acceleration profiles to minimize residual vibration after positioning operation in NC machine tools

Sato, Ryuta

Shirase, Keiichi

(Citation)
Precision Engineering,71:47-56

(Issue Date)
2021-09

(Resource Type)
journal article

(Version)
Accepted Manuscript

(URL)
https://hdl.handle.net/20.500.14094/90008386

Analytical time constant design for jerk-limited acceleration profiles to minimize residual vibration after positioning operation in NC machine tools

Ryuta Sato [1)], Keiichi Shirase [1)]

1) Department of Mechanical Engineering, Kobe University
1-1 Rokko-dai, Nada, Kobe 657-8501, JAPAN
TEL/FAX: +81-78-803-6326
Email: sato@mech.kobe-u.ac.jp

Abstract

The positioning operation of the axes of numerically controlled (NC) machine tools is essential before initiating their machining operation. Residual vibration following the positioning operations of the axes deteriorates the cycle time and quality of the machined parts. This study aims to develop a novel acceleration and deceleration design method to suppress the residual vibration during the high-speed positioning of NC machine tools. The proposed method suppresses the vibration by appropriately designing the jerk-limited acceleration profile during acceleration and deceleration. To design the jerk profile, the amplitude map that can represent the relationships between the acceleration parameters and the estimated vibration amplitude is developed. The proposed method suppresses the vibration amplitude without changing the total positioning time. To evaluate the effectiveness of this method, the residual vibration following the high-speed positioning motions was measured and simulated. The results confirm that the proposed method can effectively suppress the residual vibration.

Keywords

NC machine tools; positioning; residual vibration; vibration suppression; jerk-limited acceleration profile design

1 Introduction

Numerically controlled (NC) machine tools are a key facility in the industrial field. High speed and accuracy are essential in NC machine tools to improve the productivity and quality of the machined parts. Positioning operations are primarily required to set the relative position between the tool and the workpiece before initiating the machining operations. However, residual vibration typically occurs following the positioning operations, particularly after the higher-speed operations. Residual vibration deteriorates the productivity and surface quality of the machined parts.

A typical method to avoid the vibration is to implement a notch filter, which can decrease the gain of the system by a "notch" at the resonant frequency in the frequency domain [1]. Although the notch filter is effective in avoiding vibration and is commonly implemented in commercial NC controllers, it is difficult to apply it to suppress lower frequency vibration because it deteriorates the system response. It is known that the machine tools have a natural frequency owing to the structural vibration ranging over several ten Hertz and the vibration affects the relative motion between the tool and the workpiece [2]. Therefore, it is tedious to suppress the vibration using the notch filter even though the method is effective in suppressing higher frequency vibrations ranging over several hundred Hertz.

Another method to avoid the vibration is to apply a finite impulse response (FIR) filter to the positional commands [3]. It is well known that this filter can effectively suppress the vibration by setting the time constant to the inverse value of the vibration frequency to be suppressed. However, in suppressing the lower frequency vibration, the time constant and positioning time are increased. Posicast control [4] and input shaping [5] approaches have similar issues. Some researchers propose other vibration suppression techniques, such as the acceleration feedback technique and active vibration control systems [6–8]. However, these methods are not cost effective, as they require acceleration sensors and actuators. Sato et al. [9] proposed an active vibration suppression method that did not require any additional sensors and actuators. However, it cannot be applied to all the cases because it is tedious to oscillate the desired vibration mode in some cases.

This study proposes an effective method to suppress the residual vibration without any additional sensors and actuators, or changing the positioning time. The proposed method suppresses the vibration by appropriately designing the jerk-limited acceleration profile during acceleration and deceleration. It is generally known that jerk-limited acceleration profiles can be designed by applying an FIR filter to the original acceleration profiles. From this point of view, several studies have been carried out [10–12]. The main topic investigated in these studies is the design of an acceleration profile with jerk limitations and its application to contouring control. The vibration suppression approach through jerk-limited acceleration profiles obtained by applying FIR filters has not changed from the method mentioned in [3]. In this study, we propose a novel approach to design a jerk-limited acceleration profile that can suppress residual vibrations. To design the jerk profile, an amplitude map that represents the relationships between the

acceleration parameters and the estimated vibration amplitude was newly developed. To evaluate the effectiveness of the method, residual vibration following the high-speed positioning motions was measured and simulated.

2 Experiment and Simulation

The Z-axis of a vertical type small machining center was adopted for testing in this study. Each axis of the machining center was driven using an AC servo motor and a ball-screw. The downward motion of the Z-axis was measured and simulated in this study because Z-axis positioning is required before the initiation of machining operations. If residual vibrations exist following the motion, the machine needs to wait before proceeding to the machining operation because the vibration is directly copied onto the machined surface as striped marks. Therefore, suppression of residual vibration after the downward positioning of the Z-axis takes precedence in reducing cycle time. The positional commands during motion can be obtained from the NC controller using a monitoring function. Additionally, the desired positional command can be commanded to the axis with a 1 ms interval.

Figure 1 shows the measurement setup for the residual vibration following the positioning. The displacement between the table and spindle head was measured using a non-contact type displacement sensor (capacitance type sensor). The displacement sensor was fixed onto the table using a magnet base. It was confirmed that the measured results were not affected by the fixing method. The target position was set to the zero position and the positioning operation was started from +1 mm higher than the zero position.

Figure 2 shows the positional command and the acceleration profile during the positioning operation obtained from the controller. The acceleration profile represents the second-order derivative of the acquired positional command. The total positioning time was set to 40 ms in this study. It is evident from the figure that the acceleration changes linearly during the operation. This implies that the jerk (derivative of acceleration) was limited and had stepwise change during the operation. Jerk-limited positional command is a typical command for the axes of NC machine tools [13]. It is expected that the machine oscillated at the time of the jerk change.

In addition, simulation of the vibration was conducted. To simulate the structural vibration owing to the positioning operation, the vibration model illustrated in Figure 3 [2] was adopted in this study. It had been confirmed that the model could simulate actual vibration adequately [2, 9]. The model had 33 degrees of freedom (DOF); 6 DOF of column, head, table, saddle, and bed, and rotation of three motors for each axis. Each feed drive mechanism was modeled as 2 DOF systems, and a precise controller model was introduced.

The mass and moment of inertia of each component were obtained from the 3D CAD model. The stiffness and damping coefficients between the components were identified through matching the measured and simulated frequency responses. Figure 4 shows the measured and simulated frequency responses (mobility transfer functions) along the Z-

axis. The spindle head was oscillated using an impulse hammer along the Z-axis, and the acceleration of the head was measured to calculate the frequency response. According to the results, the measured response had several natural frequencies around 30 Hz, 50 Hz, 90 Hz, and 110 Hz. Although many natural frequencies existed, it was confirmed that the 30 Hz vibration oscillated after the positioning operations. 30 Hz, 50 Hz, 90 Hz, and 110 Hz vibrations could be observed in the simulated responses. The response around 30 Hz and 90 Hz matched with the measured response. In addition, it was confirmed that the vibration modes around 30 Hz and 90 Hz could be adequately expressed using the simulation.

After the positioning operation with the acceleration profile shown in Figure 2, the vibration at 30 Hz mainly oscillates, although the magnitude around 90 Hz is larger (as shown in Figure 4); this is because the acceleration profile shown in Figure 2 mainly has frequency components lower than 50 Hz. The vibration mode around 30 Hz was the rotational vibration of the whole machine structure around the X-axis, called the rocking mode.

3 Formulation of Jerk-Limited Acceleration Profile Design

3.1 Jerk-limited acceleration profile

Schematics of the jerk-limited acceleration profile for the positioning operations are illustrated in Figure 5. The waveform can be defined by the maximum acceleration during acceleration A_1, maximum acceleration during deceleration A_2, acceleration increasing time during acceleration T_1, acceleration decreasing time during acceleration T_2, acceleration increasing time during deceleration T_3, and acceleration decreasing time during deceleration T_4. T_{SUM} is the total positioning time and can be defined as the sum of T_1, T_2, T_3, and T_4. Figure 6 illustrates the relationship between jerk, acceleration, velocity, and displacement waveforms. According to Erkorkmaz and Altintas [13], displacement can be obtained from the constant jerk values J_1 to J_4 in each time segment T_1 to T_4.

Conventionally, the increasing and decreasing times of acceleration T_1 to T_4 are designed as identical values. However, in this study, the design method for the times T_1 to T_4 is newly proposed under the constraint of constant positioning time T_{SUM} and positioning target displacement L. To organize the design strategy, the following three conventions were compared: Condition I. $T_1 = T_2$ and $T_3 = T_4$; Condition II. $T_1 = T_3$ and $T_2 = T_4$; and Condition III. $T_1 = T_4$ and $T_2 = T_3$. Figure 7 illustrates three acceleration profile patterns investigated in this study.

3.2 Formulation of relationship between jerk and displacement

Erkorkmaz and Altintas formulated the relationship between jerk and displacement [13]. Acceleration $a(\tau)$, velocity $f(\tau)$, and displacement $s(\tau)$ can be obtained from jerk $j(\tau)$. Here, τ_i ($i = 1, 2, 3, 4$) represents the local time for the i th time segment. Jerk $j(\tau)$ for each time segment is represented as Equation (1).

$$j(\tau) = \begin{cases} J_1 & 0 \le \tau_1 < T_1 \\ J_2 & T_1 \le \tau_2 < T_2 \\ J_3 & T_2 \le \tau_3 < T_3 \\ J_4 & T_3 \le \tau_4 < T_4 \end{cases} \quad (1)$$

Acceleration for each time segment $a(\tau)$ can be obtained from the jerk as *Equation (2)*. A_1 is the initial value of $a(\tau_2)$. It can be defined by substituting T_1 as τ_1. It is clear from Figure 6 that the initial value of $a(\tau_3)$ is zero. A_2, the initial value of $a(\tau_4)$ can be defined in the same way as the initial value of $a(\tau_2)$. As the results, the maximum values of acceleration A_1 and A_2 can be represented as Equations (3) and (4).

$$a(\tau) = \begin{cases} J_1\tau_1 \\ A_1 + J_2\tau_2 \\ J_3\tau_3 \\ A_2 + J_4\tau_4 \end{cases} \quad (2)$$

$$A_1 = J_1T_1 \quad (3)$$

$$A_2 = J_3T_3 \quad (4)$$

Velocity $f(\tau)$ can be obtained by integrating Equation (2) as follows:

$$f(\tau) = \begin{cases} \frac{1}{2}J_1{\tau_1}^2 \\ f_1 + A_1\tau_1 + \frac{1}{2}J_2{\tau_2}^2 \\ f_2 + \frac{1}{2}J_3{\tau_3}^2 \\ f_3 + A_2\tau_4 + \frac{1}{2}J_4{\tau_4}^2 \end{cases}, \quad (5)$$

where f_1 to f_4 are the initial values of $f(\tau_1)$ to $f(\tau_4)$. The initial values can be obtained in the same way as in the case of the acceleration mentioned above. Velocity f_1, f_2, and f_3 can be represented as follows:

$$f_1 = \frac{1}{2}J_1{T_1}^2 \quad (6)$$

$$f_2 = f_1 + A_1T_2 + \frac{1}{2}J_2{T_2}^2 \quad (7)$$

$$f_3 = f_2 + \frac{1}{2}J_2{T_3}^2 \quad (8)$$

Similarly, displacement s (τ) can be represented as Equation (9), and the initial values s_1, s_2, and s_3 are as shown in Equations (10) to (12).

$$s(\tau) = \begin{cases} \frac{1}{6}J_1{\tau_1}^3 \\ s_1 + f_1\tau_2 + \frac{1}{2}A_1{\tau_2}^2 + \frac{1}{6}J_2{\tau_2}^3 \\ s_2 + f_2\tau_3 + \frac{1}{6}J_3{\tau_3}^3 \\ s_3 + f_3\tau_4 \frac{1}{2}A_2{\tau_4}^2 + \frac{1}{6}J_4{\tau_4}^3 \end{cases} \quad (9)$$

$$s_1 = \frac{1}{6}J_1{T_1}^3 \quad (10)$$

$$s_2 = s_1 + f_1 T_2 + \frac{1}{2} A_1 {T_2}^2 + \frac{1}{6} J_2 {T_2}^3 \tag{11}$$

$$s_3 = s_2 + f_2 T_3 + \frac{1}{6} J_3 {T_3}^3 \tag{12}$$

In addition, the positioning target displacement L can be represented by substituting T_4 to τ_4 in s_4 as Equation (13).

$$L = s_3 + f_3 T_4 + \frac{1}{2} A_2 {T_4}^2 + \frac{1}{6} J_4 {T_4}^3 \tag{13}$$

3.3 Acceleration profile under constraint of acceleration time and displacement

It is possible to define the acceleration profile based on three parameters: target displacement L, total positioning time T_{SUM}, and acceleration increasing time during acceleration T_1. In Condition III ($T_1 = T_4$ and $T_2 = T_3$), for example, the acceleration profile can be formulated as follows:

It is clear that the negative and positive areas of the acceleration profile need to be identical to have zero velocity at displacement L. Based on the constraint, the maximum acceleration A_2 should be equal to $-A_1$ because of the defined condition, $T_1 = T_4$ and $T_2 = T_3$. In addition, it is clear that jerk J_1 should be equal to J_4 and J_2 should be equal to J_3. By substituting the constraint in Equation (13), Equation (14) can be obtained as follows.

$$L = \frac{1}{3} A_1 {T_1}^2 + A_1 T_1 T_2 + \frac{2}{3} A_1 {T_2}^2 \tag{14}$$

The ratio of T_2 and T_1 is defined as R, as shown in Equation (15). Based on the definition, T_2 can be represented by Equation (16) as a function of T_1 and T_{SUM}. In addition, the ratio R can be represented by Equation (17).

$$T_2 = R T_1 \tag{15}$$

$$T_2 = \frac{T_{SUM} - 2T_1}{2} \tag{16}$$

$$R = \frac{T_{SUM} - 2T_1}{2T_1} \tag{17}$$

The target displacement L can be represented as Equation (18) by substituting Equations (15), (16), and (17) in Equation (14).

$$L = \frac{1}{6}(2R + 1) T_{SUM} A_1 T_1 \tag{18}$$

Equation (18) can be deformed to Equation (19) because acceleration A_1 is a product of J_1 and T_1. As shown in Equation (19), Jerk J_1 can be defined based on the three parameters, T_{SUM}, T_1, and L. It is also possible to define T_2 as T_4 and J_2 as J_4 based on the defined constraint.

$$J_1 = \frac{6L}{{T_1}^2 T_{SUM}(2R+1)} \tag{19}$$

Additionally, for Condition I ($T_1 = T_2$ and $T_3 = T_4$) and Condition II ($T_1 = T_3$ and $T_2 = T_4$), it is possible to represent the target displacement L based on the approach described

for Condition III. Equations (20) and (21) are the obtained results for Conditions I and II, respectively. Jerk J_1 to J_4 for other conditions can also be obtained based on the defined constraint.

$$L = \frac{1}{2} T_{SUM} A_1 T_1 \tag{20}$$

$$L = \left(\frac{1}{2} + R + \frac{1}{2}R^2\right) A_1 T_1^2 \tag{21}$$

4 Jerk-Limited Acceleration Profile Design based on Amplitude Map

4.1 Formulation of vibration amplitude

To formulate the amplitude of the oscillated vibration, a standard second-order transfer function, as shown in Equation (22), is assumed in this study. The response to the stepwise jerk change y (t) can be represented as Equation (23), as the sum of the step responses.

$$G(s) = \frac{\omega_n^2}{s^2 + 2\zeta\omega_n s + \omega_n^2} \tag{22}$$

$$\begin{aligned} y(t) = \frac{\mathrm{e}^{-\zeta\omega_n t}}{\sqrt{1-\zeta^2}} \{ & -J_1 \mathrm{e}^{-\zeta\omega_n (T_1+T_2)} \sin(\omega_d (t + T_1 + T_2) + \varphi) \\ & -(-J_1 + J_2)\mathrm{e}^{-\zeta\omega_n T_2} \sin(\omega_d (t + T_2) + \varphi) - (-J_2 + J_3) \sin(\omega_d t + \varphi) \\ & -(J_3 + J_4)\mathrm{e}^{\zeta\omega_n T_3} \sin(\omega_d (t - T_3) + \varphi) - J_4 \mathrm{e}^{\zeta\omega_n (T_3+T_4)} \sin(\omega_d (t - T_3 - T_4) + \varphi)\} \end{aligned} \tag{23}$$

where ω_d and φ are represented as Equations (24) and (25).

$$\omega_d = \sqrt{1 - \zeta^2}\,\omega_n \tag{24}$$

$$\varphi = \tan^{-1} \frac{\sqrt{1-\zeta^2}}{\zeta} \tag{25}$$

To simplify the results, the dumping ration ζ is assumed as zero in this study. Equation (23) can be simplified to Equation (26) under the assumption.

$$\begin{aligned} y(t) = \frac{1}{\omega_n} \{ & J_1 \sin \omega_n (t + T_1 + T_2) - (-J_1 + J_2) \sin \omega_n (t + T_2) - (-J_1 + J_3) \sin \omega_n t \\ & -(-J_3 + J_4) \sin \omega_n (t - T_3) + J_4 \sin \omega_n (t - T_3 - T_4)\} \end{aligned} \tag{26}$$

The amplitude of the oscillated vibration can be estimated based on Equation (26) for each condition. For example, for the amplitude in Condition III ($T_1 = T_4$ and $T_2 = T_3$), jerk $J_4 = J_1$, and jerk $J_2 = J_3$. Therefore, jerk J_2 can be represented as a function of J_1 based on the ratio R as follows:

$$J_2 = -\frac{1}{R} J_1 \tag{27}$$

By substituting the relationships between the constants of Equation (26), the vibration amplitude, *Amp* can be obtained as Equation (28) from Equation (26) for Condition III.

$$Amp = \frac{2J_1}{\omega_n}\{\left(1+\frac{1}{R}\right)\sin\omega_n RT_1 - \sin\omega_n\frac{T_{SUM}}{2}\} \quad (28)$$

The ratio R can be represented as a function of T_{SUM} and T_1, as shown in Equation (17) for all the conditions. This implies that the amplitude of the oscillated vibration can be expressed as a function of J_1, T_{SUM}, and T_1 for any natural angular frequency ω_n and displacement L. Table 1 presents the estimated amplitude of the oscillated vibration for each condition.

4.2 Amplitude map

It has been shown that the amplitude of the oscillated vibration following the positioning operation can be represented as a function of acceleration increasing time during acceleration T_1, total positioning time T_{SUM}, positioning target displacement L, and angular natural frequency ω_n (=$2\pi f$). Hence, it is possible to represent the amplitude as a function of T_1 and T_{SUM} under constant displacement L and vibration frequency f. This implies that the optimum relationship between T_1 and T_{SUM} can be designed based on the estimated vibration amplitude for each displacement L and frequency f.

In this study, a novel amplitude map that can represent the change in amplitude as a function of T_1 and T_{SUM} has been proposed based on the amplitude analysis mentioned above. The horizontal and vertical axes of the map are T_1 and T_{SUM}, respectively. Target displacement L is set to 1 mm and the frequency f is set to 30 Hz.

The generated amplitude maps for the three conditions are shown in Figures 8. Figure 8 (a) shows the map for Condition I ($T_1 = T_2$ and $T_3 = T_4$), Figure 8 (b) shows the map for Condition II ($T_1 = T_3$ and $T_2 = T_4$), and Figure 8 (c) shows the map for Condition III ($T_1 = T_4$ and $T_2 = T_3$). The color of the map indicates the amplitude. The trend of change in the amplitude depends on these conditions. The maximum value of T_1 is limited to $T_{\mathrm{SUM}}/2$. Therefore, the bottom right area of the map (white area) is not applicable.

According to Figure 8, the vibration amplitude becomes smaller by expanding the total positioning time T_{SUM}, as generally known for all conditions. In contrast, regarding the influence of T_1, a shorter T_1 makes smaller vibrations only in Condition III, as shown in Figure 8 (c). This means that the vibration can be suppressed by changing T_1 without any change in the total acceleration time T_{SUM}. Under other conditions, Conditions I and II, the vibration amplitude is not significantly affected by changing T_1, as shown in Figure 8 (a) and (b). These results suggest that only Condition III can reduce residual vibrations by shortening the acceleration increasing time during acceleration T_1, under the constraint of the constant total positioning time T_{SUM}.

5. Effect of the Proposed Jerk-Limited Acceleration Profile Design Method

As mentioned above, residual vibrations can be reduced by shortening the acceleration increasing time during acceleration T_1 through Condition III. To confirm the

effect of changing T_1, Condition III is adopted, and measurement and simulation of a positioning operation are carried out. Figure 9 shows the conventional and designed acceleration profiles; Figure 9 (a) shows the conventional acceleration profile, and Figure 9 (b) shows the designed acceleration profile based on the proposed amplitude map. Although the total positioning time T_{SUM} was fixed at 40 ms, the acceleration-increasing time during acceleration T_1 was set to 1 ms. The smallest value of T_1 was limited using the control command interval. According to the amplitude map shown in the figure, it is expected that the designed acceleration profile can reduce the amplitude of residual vibration. It should be noted that the servo system cannot follow commands. The residual vibrations are suppressed based on the relationship between the input command and response of the system.

Figure 10 shows the simulated residual vibration with and without an amplitude map-based acceleration profile design. Figure 10 (a) shows the result with the conventional acceleration profile, and Figure 10 (b) shows the result with the designed acceleration profile based on the acceleration map. It is evident from the results that the designed acceleration profile can significantly suppress the 30 Hz residual vibration. This is also evident from the frequency analysis of the vibration shown in Figure 10 (c).

Figure 11 shows the measured residual vibration with and without an amplitude map-based acceleration profile design. Figure 11 (a) shows the result with the conventional acceleration profile, and Figure 11 (b) shows the result with the designed acceleration profile based on the acceleration map. It can be confirmed that the residual vibration can be suppressed by designing the acceleration profile based on the amplitude map.

According to the frequency analysis of the vibration shown in Figure 11 (c), the higher-frequency component can be observed in the results. Figure 12 shows the frequency analysis results of the acceleration profiles. The amplitude at 30 Hz reduces for the acceleration profile designed based on the acceleration map. However, the designed acceleration profile has higher-frequency components, which yields the higher-frequency components of the residual vibrations. The design strategy for vibrations with several frequencies will be studied in future work.

6. Conclusion

This study proposes an effective method to suppress the residual vibration without any additional sensors or actuators, and change in the positioning time. In this study, a method to suppress the vibration by appropriately designing the jerk-limited acceleration profile during acceleration and deceleration is proposed. To design the jerk profile, the amplitude map that can represent the relationships between the acceleration parameters and estimated vibration amplitude is proposed. The conclusions of this study can be summarized as follows:

(1) Amplitude of the oscillated vibration can be expressed as a function of J_1, T_{SUM}, and T_1 for any natural angular frequency ω_n and displacement L.

(2) The optimum relationship between T_1 and T_{SUM} can be designed based on the estimated vibration amplitude for each displacement L and frequency f.
(3) Residual vibration can be reduced significantly using the proposed jerk-limited acceleration profile design method based on proposed amplitude map.

Although the simulations and experiments of the downward motions were carried out for the Z-axis, the proposed amplitude map does not depend on the axis and direction of motion. This means that the proposed method can generally be applied to other axes and directions. We will attempt to confirm the effectiveness of the proposed method in other feed drives and positioning motions. In the future, we will also attempt to develop a design strategy for vibrations with several frequencies.

Acknowledgements

The authors would like to acknowledge the significant contribution of Miss. Nishijima, an undergraduate student of Kobe University, toward the experiments and simulations.

Reference

[1] Kuo, B.C., Frequency-domain design of control systems, Automatic Control Systems, 6th ed.; Prentice-Hall International: New Jersey, USA, 1991, pp. 664-720.
[2] Sato, R., Tashiro, G., Shirase, K., Analysis of the coupled vibration between feed drive systems and machine tool structure, Int. J. Auto. Technol., 9, 2015, 689-697.
[3] Chen, C.-S., Lee, A.-C., Design of acceleration/deceleration profiles in motion control based on digital FIR filters, Int. J. Mach. Tools Manuf., 38, 1998, 799-825.
[4] Smith, O.J.M., Posicast control of dumped oscillatory systems, Proc. of IRE, 45, 1957, 1249-1255.
[5] Singer, N.C., Seering, W.P., Preshaping command inputs to reduce system vibration, ASME J. Dyna. Syst. Meas. Cont., 112, 1990, 76-82.
[6] Kai, T., Sekiguchi, H., Ikeda, H., Relative vibration suppression in a positioning machine using acceleration feedback control, IEEJ J. Ind. Appl., 7, 2018, 15-21.
[7] Denkena, B., Eckl, M., Lepper, T., Advanced control strategies for active vibration suppression in laser cutting machines, Int. J. Auto. Technol., 9, 2015, 425-435.
[8] Zaeh, M.F., Kleinwort, R., Fagerer, P., Altintas, Y., Automatic tuning of active vibration control systems using inertial actuators, CIRP Ann. - Manuf. Technol., 66, 2017, 365-368.
[9] Sato, R., Hayashi, H., Shirase, K., Active vibration suppression of NC machine tools for high-speed contouring motions. J. Adv. Mech. Des., Syst., Manuf., 14, 2020, No.19-00274.
[10] Besset, P., Bearee, R., FIR filter-based online jerk constrained trajectory generation, Cont. Eng. Prac., 66, 2017, 169-180.
[11] Sencer, B., Altintas, Y., Croft, E., Feed optimization for five-axis CNC machine tools with drive constraints, Int. J. Mach. Tools Manuf., 48, 2008, 733-745.
[12] Tajima, S., Sencer, B., Shamoto, E., Accurate interpolation of machining too-paths based on

FIR filtering, Prec. Eng., 51, 2018, 332-344.
[13] Erkorkmaz, K., Altintas, Y., High speed CNC design. Part I: Jerk limited trajectory generation and quantic spline interpolation, Int. J. Mach. Tools Manuf., 41, 2001, 1323-1345.

Figures:

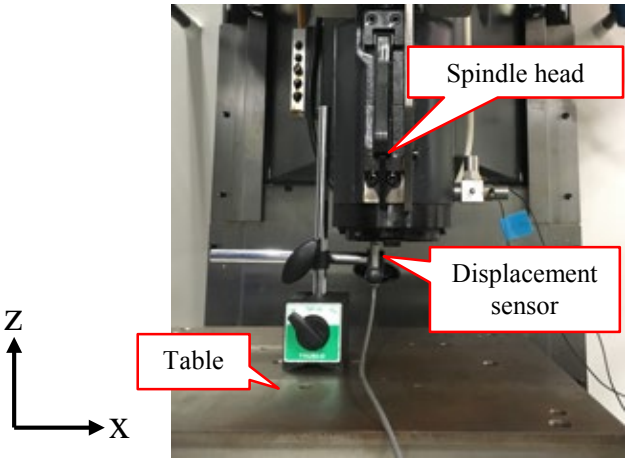

Figure 1. Measurement setup for residual vibration of the downward positioning operation of the Z-axis using a non-contact type displacement sensor.

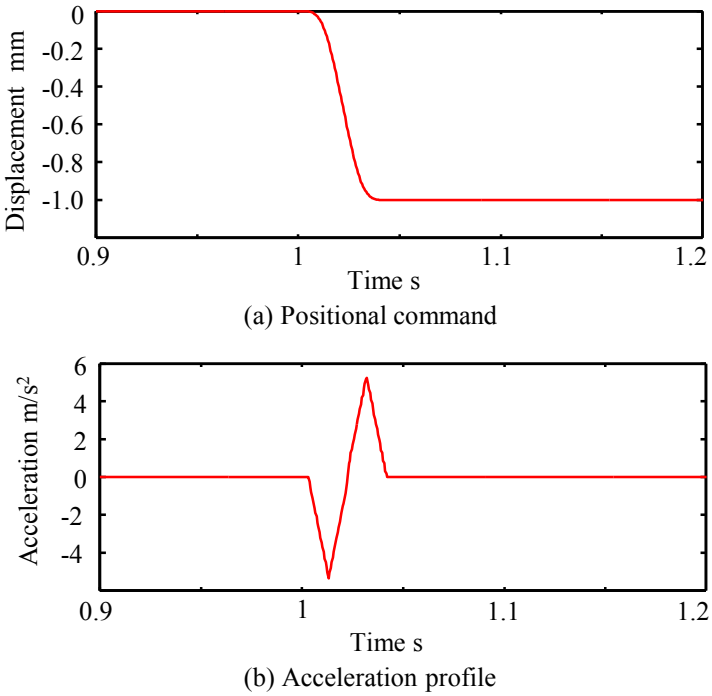

Figure 2. Positional command and acceleration profile during the positioning operation

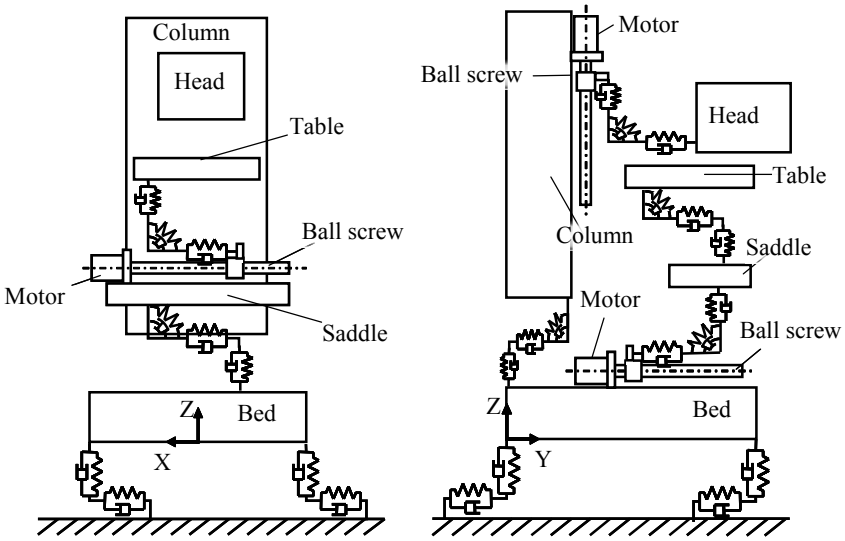

(a) Z-X plane view (b) Y-Z plane view

Figure 3. Vibration model of machine tool structure with 33 DOF [2]

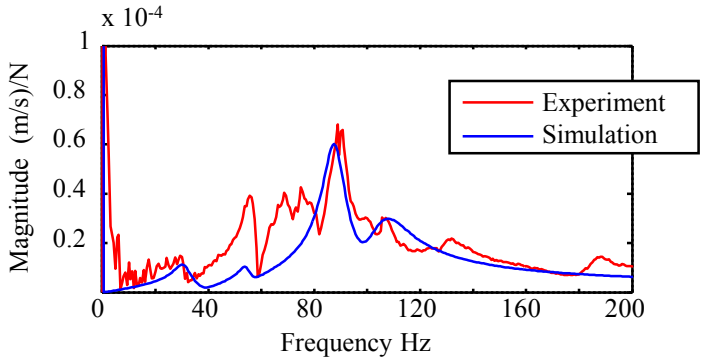

Figure 4. Comparison of measured and simulated frequency responses along Z-axis.

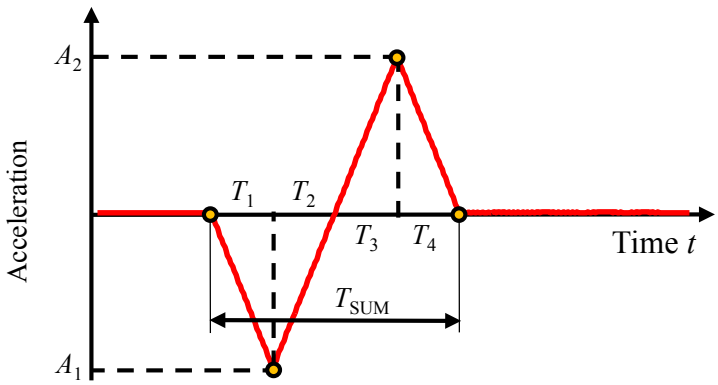

Figure 5. Jerk-limited acceleration profile for positioning operations.

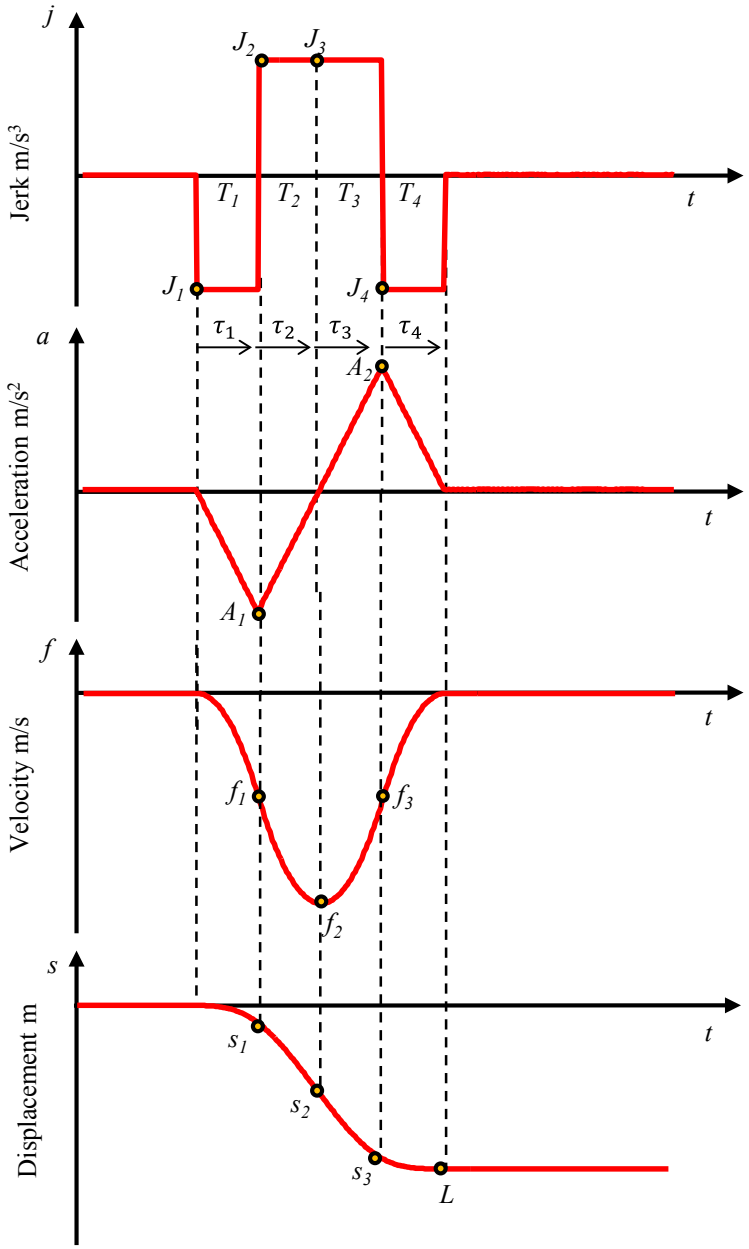

Figure 6. Jerk, acceleration, velocity, and displacement wave forms during positioning operation.

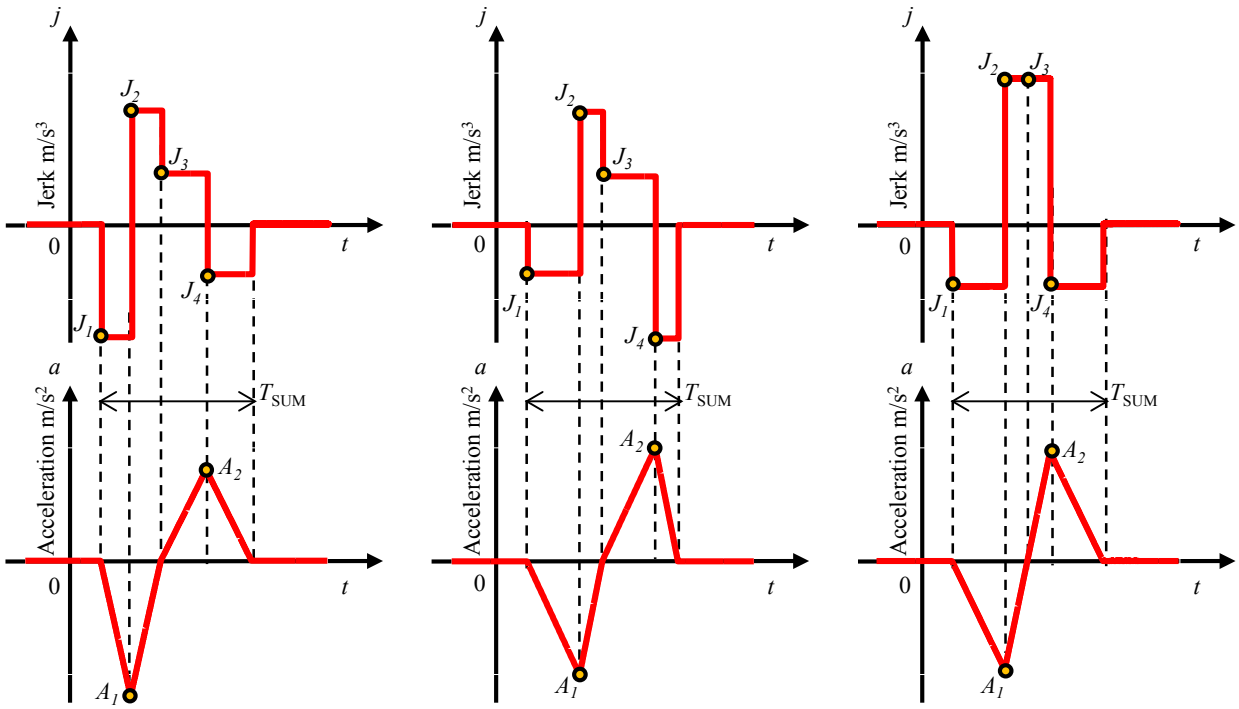

(a) T_1=T_2, T_3=T_4 (Condition I) (b) T_1=T_3, T_2=T_4 (Condition II) (c) T_1=T_4, T_2=T_3 (Condition III)

Figure 7. Schematics of jerk and acceleration profiles investigated in this study.

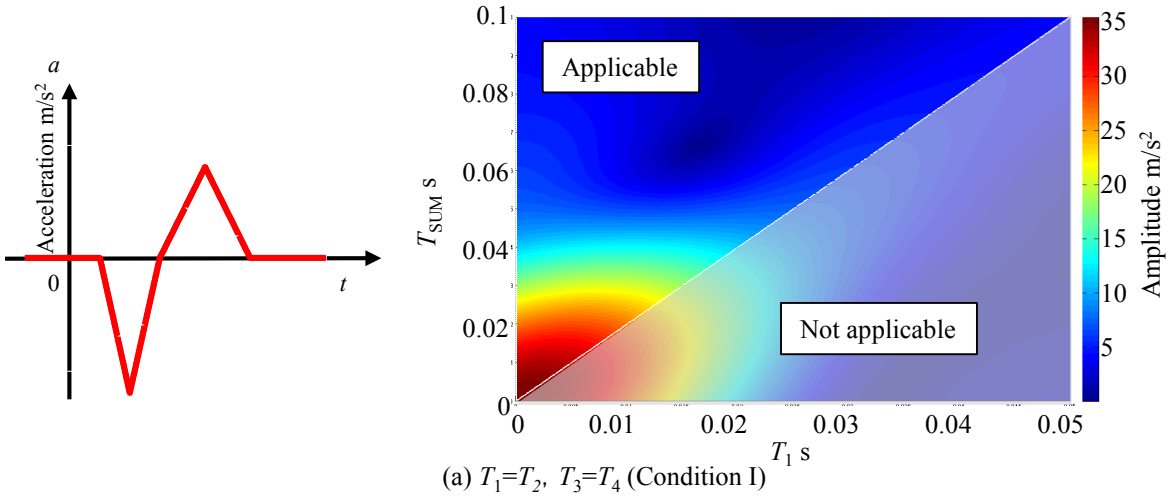

(a) T_1=T_2, T_3=T_4 (Condition I)

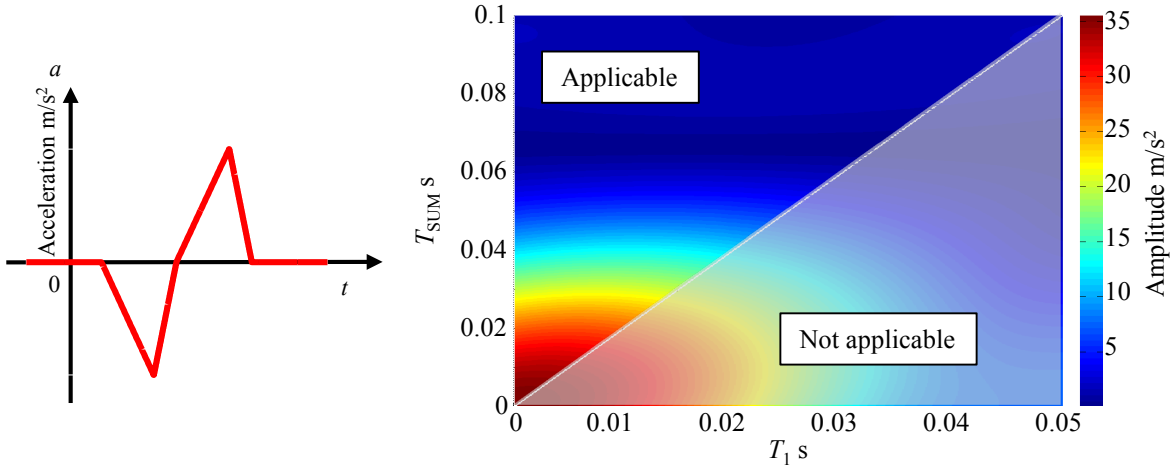

(b) T_1=T_3, T_2=T_4 (Condition II)

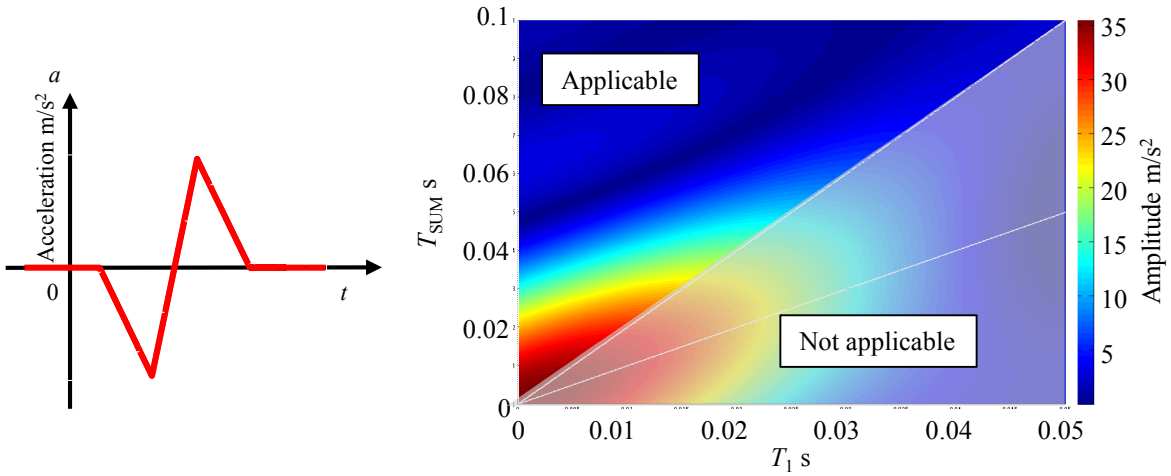

(c) T_1=T_4, T_2=T_3 (Condition III)

Figure 8. Proposed amplitude map to design jerk-limited acceleration profile for 1 mm displacement and 30 Hz vibration

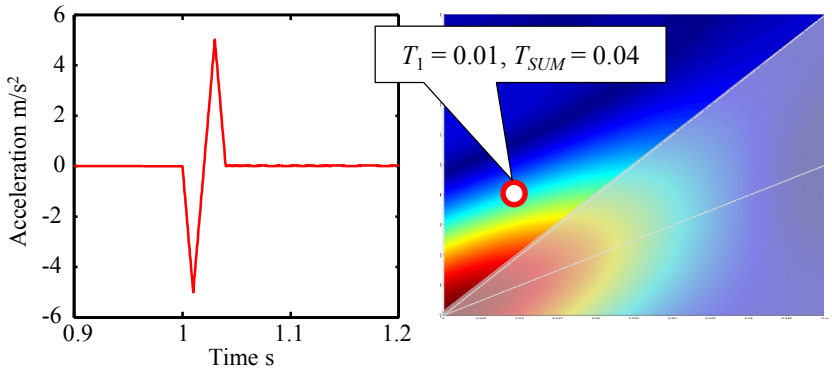

(a) Conventional acceleration profile

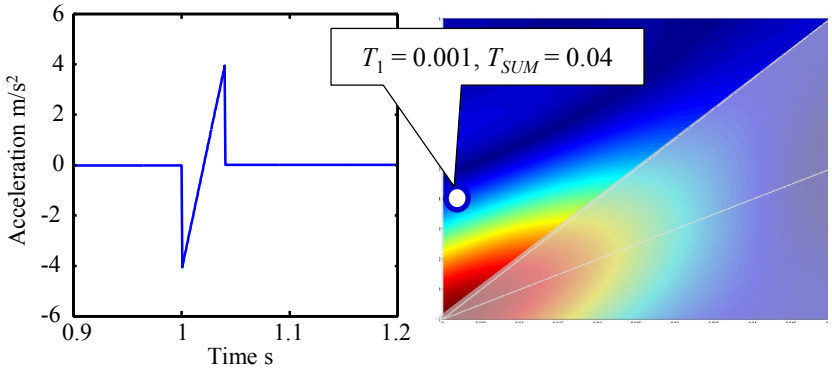

(b) Designed acceleration profile based on proposed amplitude map

Figure 9. Conventional and designed acceleration profiles for measurement and simulation.

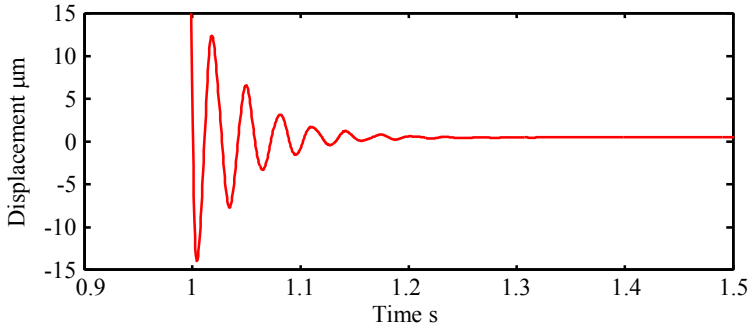

(a) Conventional acceleration profile (T_1 = 0.01, T_{SUM} = 0.04)

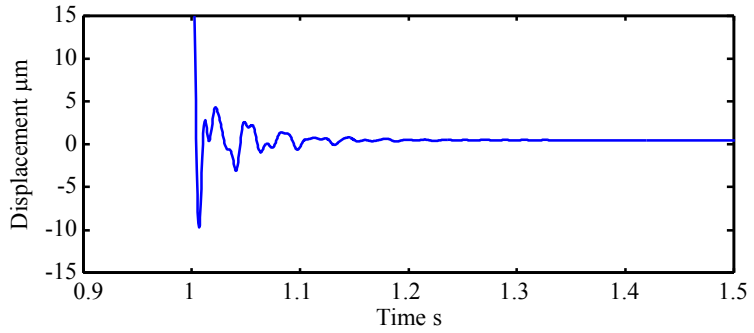

(b) Designed acceleration profile (T_1 = 0.001, T_{SUM} = 0.04)

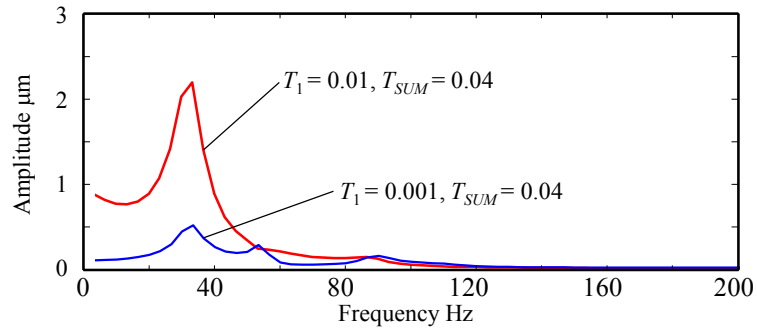

(c) Frequency analysis

Figure 10. Simulated residual vibration after positioning operation.

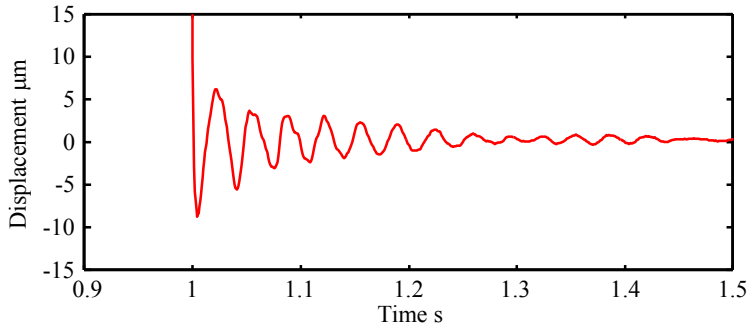

(a) Conventional acceleration profile (T_1 = 0.01, T_{SUM} = 0.04)

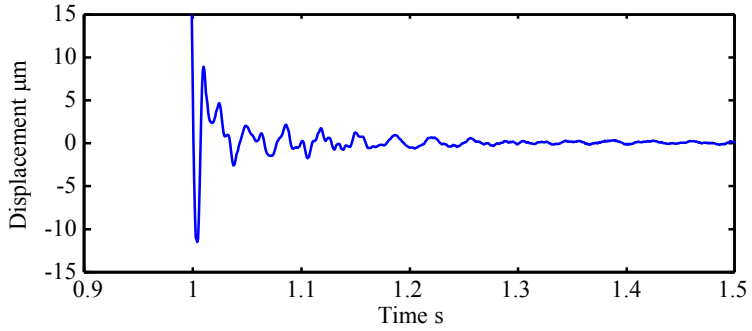

(b) Designed acceleration profile (T_1 = 0.001, T_{SUM} = 0.04)

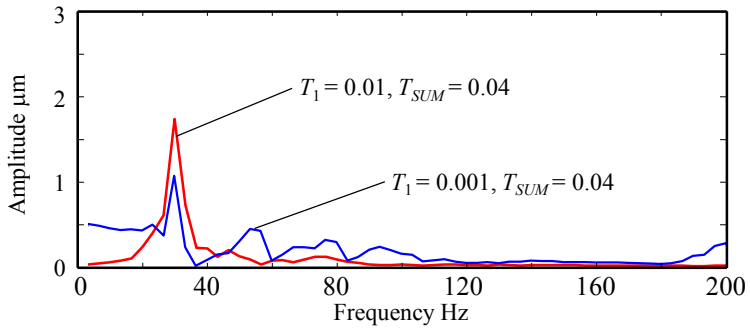

(c) Frequency analysis

Figure 11. Measured residual vibration after positioning operation.

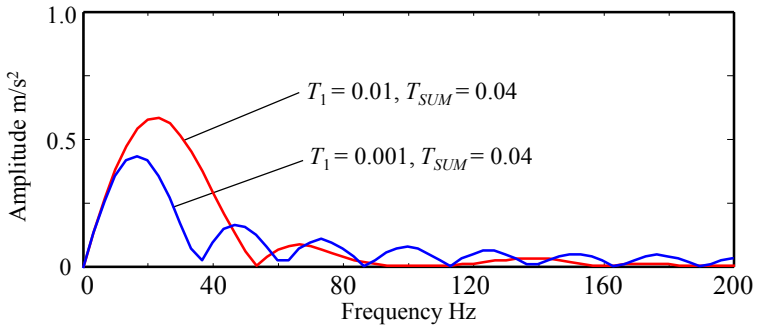

Figure 12. Comparison of frequency analysis results of the acceleration profiles.

Table:

Table 1. Dependence of estimated vibration amplitude on acceleration waveform conditions.

$T_1 = T_2$	$\frac{J_1}{\omega_n}\sqrt{\left(-\cos 2\omega_n T_1 + 2\cos\omega_n T_1 - \frac{2}{R^2}\cos R\omega_n T_1 + \frac{1}{R^2}\cos 2R\omega_n T_1 - \left(1-\frac{1}{R^2}\right)\right)^2 + \left(-\sin 2\omega_n T_1 + 2\sin\omega_n T_1 + \frac{2}{R^2}\sin R\omega_n T_1 - \frac{1}{R^2}\sin 2R\omega_n T_1\right)^2}$
$T_1 = T_3$	$\frac{J_1}{\omega_n}\sqrt{\left\{\left(-1+\frac{1}{R}\right)\cos\omega_n(1+R)T_1 - \left(-1-\frac{1}{R}\right)\cos\omega_n RT_1 - \left(1+\frac{1}{R}\right)\cos\omega_n T_1 - \left(-1+\frac{1}{R}\right)\right\}^2 + \left\{\left(-1-\frac{1}{R}\right)\sin\omega_n(1+R)T_1 - \left(-1-\frac{1}{R}\right)\sin\omega_n RT_1 + \left(1+\frac{1}{R}\right)\sin\omega_n T_1\right\}^2}$
$T_1 = T_4$	$\frac{2J_1}{\omega_n}\left\{\left(1+\frac{1}{R}\right)\sin\omega_n RT_1 - \sin\omega_n\frac{T_{SUM}}{2}\right\}$